

LARGE-SCALE ENVIRONMENTAL EFFECTS OF THE CLUSTER DISTRIBUTION

Manolis Plionis

Institute of Astronomy & Astrophysics, National Observatory of Athens, Lofos Koufou, Palaia Penteli, 152 36 Athens, Greece

plionis@sapfo.astro.noa.gr

Abstract Using the APM cluster distribution we find interesting alignment effects: (1) Cluster substructure is strongly correlated with the tendency of clusters to be aligned with their nearest neighbour and in general with the nearby clusters that belong to the same supercluster, (2) Clusters belonging in superclusters show a statistical significant tendency to be aligned with the major axis orientation of their parent supercluster. Furthermore we find that dynamically young clusters are more clustered than the overall cluster population. These are strong indications that cluster develop in a hierarchical fashion by merging along the large-scale filamentary superclusters within which they are embedded.

Keywords: galaxies: clusters - cosmology: general - large-scale structure of universe

1. Introduction

Galaxy clusters are very important for Cosmological studies because: (a) being the largest bound structures in the universe and containing hundreds of galaxies and hot X-ray emitting gas, they can be detected at large distances; (b) they are closed systems with a mixture of matter which is representative of the whole Universe. Therefore, they appear to be ideal tools for studying the relative abundance of different types of matter and for testing theories of structure formation (cf. Böhringer [7], Schindler [31], Borgani & Guzzo [6]).

Below I discuss a few issues related to cluster dynamics and the cluster large-scale environment and by using the APM cluster catalogue (Dalton *et al* [9]) I will present evidence that the are closely related.

1.1. Cluster Internal Dynamics & Cosmology

One of the interesting properties of galaxy clusters is the relation between their dynamical state and the underlying cosmology. Although the physics of cluster formation is complicated (cf. Sarazin [29]), it is expected that in an open or a flat with vacuum-energy contribution universe, clustering effectively freezes at high redshifts (for example in an open model, $z \simeq \Omega_m^{-1} - 1$) and thus clusters today should appear more relaxed with weak or no indications of substructure. Instead, in a critical density model, such systems continue to form even today and should appear to be dynamically active (cf. Richstone, Loeb & Turner [25], Evrard *et al.* [11], Lacey & Cole [16]). Therefore by studying the relative evolution of cluster physical properties, between distant and nearby clusters, one can attempt to extract cosmological information.

Such a task is however hampered by, at least, two facts:

- *Ambiguity in identifying cluster substructure:* One has to deal with the issue of unambiguously identifying cluster substructure, since projection effects in the optical can conspire to make cluster images appear having multiple peaks/substructure. A lot of work has been devoted in attempts to find criteria and methods to identify cluster substructure (see references in Kolokotronis *et al* [15]). It is evident from all the available studies that there is neither agreement on the methods utilised nor on the exact frequency of clusters having substructure.
- *Unknown physics of cluster merging:* The clear-cut theoretical expectations regarding the fraction of clusters expected to be relaxed in different cosmological backgrounds break-down due to the complicated physics of cluster merging (cf. Sarazin [29]) and especially due to the uncertainty of the post-merging relaxation time. In other words, identifying a cluster with significant substructure does not necessarily mean that this cluster is dynamically young, but could reflect a relatively ancient merging that has not relaxed yet to an equilibrium configuration.

It has been realized that the optimum approach in detecting clusters and studying their dynamical state is by using multiwavelength data. For example, the cluster X-ray emission is proportional to the square of the gas density (rather than just density in the optical) and therefore it is centrally concentrated, a fact which minimises projection effects (cf. Sarazin [28], Schindler [30]). The advantage of using optical data is the sheer size of the available cluster catalogues and thus the statistical significance of the emanating results. However, as we discussed previously,

it seems that in order to take advantage of the different rates of cluster evolution in the different cosmological backgrounds one needs (a) to find criteria of recent cluster merging and (b) calibrate the results using high-resolution cosmological hydro simulation, which will provide the expectations of the different cosmological models.

Such criteria have been born out of numerical simulations (cf. Roettiger *et al.* [26] [27]) and are based on the use of multiwavelength data, especially optical and X-ray data but radio as well (cf. Zabludoff & Zaritsky [41], Schindler [30]). The criteria are based on the fact that gas is collisional while galaxies are not and therefore during the merger of two clumps, containing galaxies and gas, we expect: (1) a difference in the spatial positions of the highest peak in the galaxy and gas distribution, (2) the X-ray emitting gas, due to compression along the merging direction, to be elongated perpendicularly along this direction and (3) temperature gradients to develop due to the compression and subsequent shock heating of the gas.

1.2. Cluster Alignments & Formation Processes

Another interesting observable, that was thought initially to provide strong constraints on theories of galaxy formation, is the tendency of clusters to be aligned with their nearest neighbour as well as with other clusters that reside in the same supercluster (cf. Binggeli [3], West [37], Plionis [22]). Analytical work of Bond [4] [5] in which clusters were identified as peaks of an initial Gaussian random field, has shown that such alignments, expected naturally to occur in "top-down" scenarios, are also found in hierarchical clustering models of structure formation like the CDM. These results were corroborated with the use of high-resolution N-body simulations by West *et al* [38], Splinter *et al* [33] and Onuora & Thomas [21]. This fact has been explained as the result of an interesting property of Gaussian random fields that occurs for a wide range of initial conditions and which is the "cross-talk" between density fluctuations on different scales. This property is apparently also the cause of the observed filamentariness observed not only in "pancake" models but also in hierarchical models of structure formation; the strength of the effect, however, differs from model to model.

There is strong evidence that the brightest galaxy (BCGs) in clusters are aligned with the orientation of their parent cluster and even with the orientation of the large-scale filamentary structure within which they are embedded (cf. Struble [34], West [39], Fuller, West & Bridges [12]). Furthermore, there is conflicting evidence regarding the alignment of cluster galaxies in general with the orientation of their parent cluster (cf.

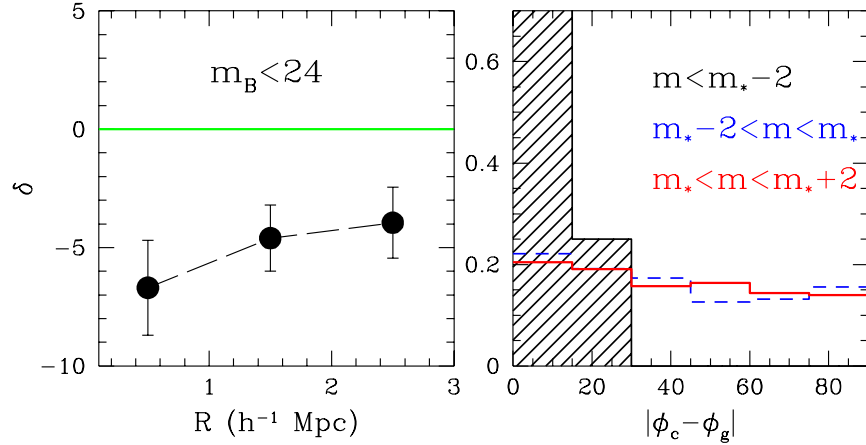


Figure 1. Left: The alignment signal of all galaxies within $3 h^{-1}$ Mpc of the cD galaxy of A521 as a function of distance from it. Right: Frequency distribution of the misalignment angle between member galaxy and A521 orientations for 3 magnitude bins.

Djorgovski [8], van Kampen & Rhee [14], Trevese, Cirimele & Flin [36]). It may be that general galaxy alignments may be present in forming, dynamically young, clusters, while in relaxed clusters violent and other relaxation processes may erase such alignment features. Such seems to be the case of the Abell 85/87/89 complex (see Durret *et al* [10]) and of Abell 521, a cluster at $z \simeq 0.25$ which is forming at the intersection of two filaments (Arnaud *et al* [1]).

Using wide-field CFHT imaging data of A521, Plionis, Maurogordato & Benoist (*in preparation*) have found statistical significant alignments not only of the predominantly bright but also of fainter galaxies with the major axis direction of the cluster (figure 1). It is interesting that the Position angle of the cluster coincides with the direction to the nearest Abell cluster (see figure 2). Within the framework of hierarchical clustering, the anisotropic merger scenario of West [39], in which clusters form by accreting material along the filamentary structure within which they are embedded, provides an interesting explanation of such alignments as well as of the observed strong alignment of BCGs with their parent cluster orientation. Evidence supporting this scenario was presented in West, Jones & Forman [40] in which they found, using Einstein data, that cluster substructures seem to be aligned with the orientation of their parent cluster and with the nearest-neighbouring cluster (see

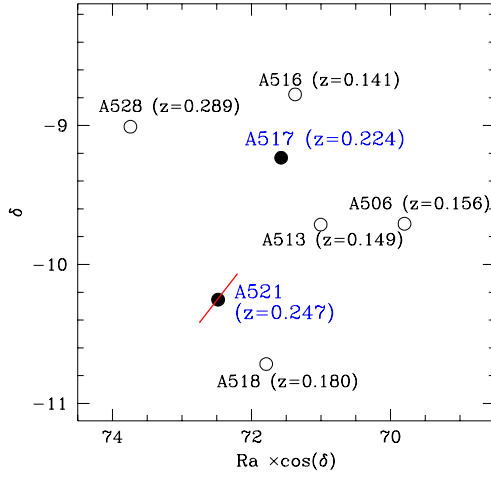


Figure 2. The large scale environment surrounding Abell 521. The major axis direction of A521 is pointing towards its nearest neighbour A517.

also Novikov *et al* [20]). Such effect has been observed also in numerical simulations of cluster formation for a variety of power-spectra (van Haarlem & van de Weygaert [13])

2. Methodology

The APM cluster catalogue is based on the APM galaxy survey which covers an area of 4300 square degrees in the southern sky containing about 2.5 million galaxies brighter than a magnitude limit of $b_J = 20.5$ (for details see Maddox *et al.* [18]). Dalton *et al.* [9] applied an object cluster finding algorithm to the APM galaxy data using a search radius of $0.75 h^{-1}$ Mpc in order to minimize projection effects, and so produced a list of 957 clusters with $z_{est} < 0.13$. Out of these 309 ($\sim 32\%$) are ACO clusters, while 374 ($\sim 39\%$) have measured redshifts (179 of these are ACO clusters). The APM clusters that are not in the ACO list are relatively poorer systems than the Abell clusters, as we have verified comparing their APM richness's.

Below, I briefly present the methods used to determine the dynamical state of clusters, their shape, orientation and alignment.

2.1. Substructure Measures

As our indicator of cluster substructure of the optical APM data we use the shift of the center-of-mass position as a function of density threshold above which it is estimated, sc (cf. Evrard *et al.* [11] and Mohr *et al.* [19]). Kolokotronis *et al* [15], used APM and X-ray (ROSAT pointed observations) data for 22 clusters and calibrated this method.

Only in $\sim 20\%$ of the clusters that they studied did they find projection effects in the optical that altered the X-ray definition of substructure. They concluded that a large and significant value of center-of-mass shift is a clear indication of substructure in the optical APM data (see also Plionis [23]).

The significance of the centroid variations to the presence of background contamination and random density fluctuations are quantified using Monte Carlo cluster simulations in which, by construction, there is no substructure. For each APM cluster a series of simulated clusters is produced having the same shape parameters, same number of observed galaxies as well as a random distribution of background galaxies, determined by the distance of the cluster and the APM selection function. The simulated galaxy distribution follows the usual King-like profile, which characterizes equilibrium configurations. Naturally, we expect the simulated clusters to generate small sc 's and in any case insignificant shifts. Therefore, for each optical cluster, 1000 such Monte-Carlo clusters are generated and we derive $\langle sc \rangle_{\text{sim}}$ as a function of the same density thresholds as in the real cluster case. Then, we calculate the quantity:

$$\sigma = \frac{\langle sc \rangle_o - \langle sc \rangle_{\text{sim}}}{\sigma_{\text{sim}}}, \quad (1)$$

where $\langle sc \rangle_o$ is the centroid shift of the real APM cluster. σ is a measure of the significance of real centroid shifts as compared to the simulated, substructure-free clusters, having the same structural and density parameters as the real cluster.

A further possible substructure identification procedure is based on a friend-of-friends algorithm, applied on 3 overdensity thresholds of each cluster (for details see Kolokotronis *et al.* [15]. Three categories are identified, based on the subgroup multiplicity and size: (a) No substructure (unimodal), (b) Weak substructure (multipole groups but with total group mass $\leq 25\%$ of main), (c) Strong substructure (multipole groups but with mass $> 25\%$ of main).

2.2. Shape & Alignment Measures

To estimate the cluster parameters we use the familiar moments of inertia method, with $I_{11} = \sum w_i(r_i^2 - x_i^2)$, $I_{22} = \sum w_i(r_i^2 - y_i^2)$, $I_{12} = I_{21} = -\sum w_i x_i y_i$, where x_i and y_i are the Cartesian coordinates of the galaxies and w_i is their weight. We, then diagonalize the inertia tensor solving the basic equation:

$$\det(I_{ij} - \lambda^2 M_2) = 0, \quad (2)$$

where M_2 is the 2×2 unit matrix. The cluster ellipticity is given by $\epsilon = 1 - \frac{\lambda_2}{\lambda_1}$, where λ_i are the positive eigenvalues with ($\lambda_1 > \lambda_2$).

This method can be applied to the data using either the discrete or smoothed distribution of galaxies (for details see Basilakos, Plionis & Maddox [2]).

In order to test whether there is any significant bias and tendency of the position angles to cluster around particular values we estimate their Fourier transform: $C_n = \sqrt{(2/N)} \sum \cos 2n\theta$, $S_n = \sqrt{(2/N)} \sum \sin 2n\theta$. If the cluster position angles, θ , are uniformly distributed between 0° and 180° , then both C_n and S_n have zero mean and unit standard deviation. Therefore large values (> 2.5) indicate significant deviation from isotropy.

In order to investigate the alignment between cluster orientations, we define the relative position angle between cluster pairs by, $\delta\phi_{i,j} \equiv |\theta_i - \theta_j|$. In an isotropic distribution we will have $\langle \delta\phi_{i,j} \rangle \simeq 45^\circ$. A significant deviation from this would be an indication of an anisotropic distribution which can be quantified by (Struble & Peebles [35]):

$$\delta = \sum_{i=1}^N \frac{\delta\phi_{i,j}}{N} - 45 \quad (3)$$

In an isotropic distribution we have $\langle \delta \rangle \simeq 0$, while the standard deviation is given by $\sigma = 90/\sqrt{12N}$. A significantly negative value of δ would indicate alignment and a positive misalignment.

3. APM Cluster Substructure & Alignments

Applying the above methodology to the ~ 900 APM clusters we find that about 30% of clusters have significant ($> 3\sigma$) substructure. Note that defining as having significant substructure those clusters with $\sigma > 2$ or 2.5 increases the fraction to $\sim 50\%$ and 40% respectively. Alternatively, if we apply the *subgroup* categorization procedure we find that $\sim 53\%$ of the APM clusters show strong indications of substructure, which would point that, for consistency among the two methods, a limit of $\sigma \simeq 2.5$ would be required above which substructure should be considered significant.

A necessary prerequisite for alignment analyses is that there is no orientation bias in the distribution of estimated position angles. In the lower panel of figure 3 we present the corresponding distribution for the APM clusters. It is evident that the distribution is isotropic, as it is also quantified by the Fourier analysis. In the upper-panel of figure 3 we present the distribution of relative position angles, $\delta\phi$, between APM nearest-neighbours for two separation limits (one for all separations and

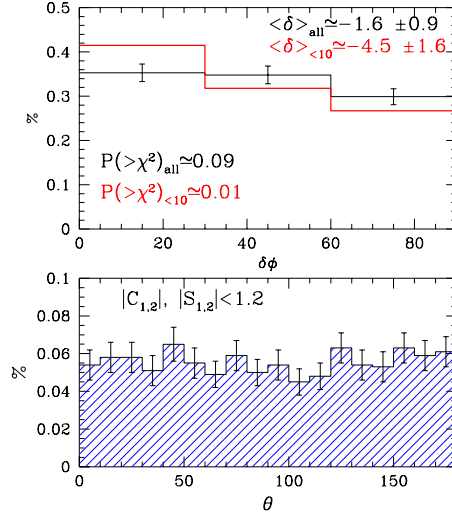


Figure 3. Upper panel: The distribution of relative position angles between nearest-neighbours. Lower panel: The distribution of APM cluster position angles. No orientation bias is present, as seen from the small values of their Fourier transforms.

one for separations $< 10 h^{-1}$ Mpc). It is evident that there is significant indication of cluster alignments in the small separation limit.

In order to test whether this result is dominated by the ACO cluster pairs, and thus whether it is a manifestation of the already known Abell cluster alignment effect (cf. Bingelli [3]; Plionis [22]), we have excluded such pairs to find not only consistent results but an even stronger alignment signal.

Furthermore, we have correlated the alignment signal with the substructure significance indication in order to see whether there is any relation between the large-scale environment, in which the cluster distribution is embedded, and the internal cluster dynamics. In figure 4 we present the alignment signal, $\langle\delta\rangle$, between cluster nearest-neighbours (filled dots) and between all pairs (open dots) with pair separations $< 20 h^{-1}$ Mpc. There is a strong correlation between the strength of the alignment signal and the substructure significance level (see for details Plionis & Basilakos [24]).

Note that from the analysis of Kolokotronis *et al.* [15] it is expected that our procedure will misidentify the dynamical state of $\sim 20\%$ of the APM clusters. However, such misidentification will act as noise and will tend to smear any true alignment-substructure correlation, since there is no physical reason why random projection effects, within $0.75 h^{-1}$ Mpc of the cluster core, should be correlated with the direction of neighbours within distances up to a few tens of Mpc's (such a correlation could be expected at some level only for nearest-neighbours in angular space but

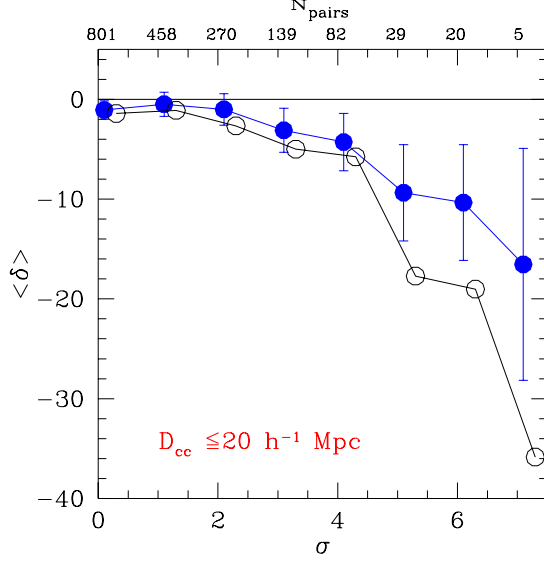


Figure 4. Alignment signal of all cluster pairs with separation $D_{cc} \leq 20 h^{-1} \text{ Mpc}$, as a function of substructure significance, σ . The filled symbols represent the signal based only on the *centroid-shift* substructure categorization while the open symbols represent the signal from clusters that are also categorized as having *strong* substructure by the *subgroup* categorization procedure.

we have verified that by choosing such pairs we obtain an insignificant alignment signal).

4. Cluster Substructure *vs* Local Density

Our previous results support the formation of clusters by anisotropic merging along the filamentary structure within which they are embedded (cf. West [39] [40]). If this view is correct then one would expect that clusters with significant substructure should also reside, preferentially, in high-density environments (superclusters), and this should then have an imprint in their spatial two-point correlation function. In the upper panel of figure 5 we present the spatial 2-point correlation function of all APM clusters (open dots) and of those with substructure significance $\sigma \geq 4$ (red dots). It is clear that the latter are significantly more clustered. This can be seen also in the insert of figure 5 where we plot the correlation length, r_0 , as a function of σ , which is clearly an increasing function of cluster substructure significance level. To test whether this effect could be due to the well-known richness dependence of the correlation strength, we investigated the mean APM richness as a function of σ and verified that if any, there is only a small such richness trend. The conclusion of this correlation function analysis is that indeed the clusters showing evidence of dynamical activity reside in high-density environments, as anticipated from the alignment analysis. It is interesting that such environmental dependence has also been found in a similar study of the BCS and REFLEX clusters (Schücker *et al.*, [32]) and for

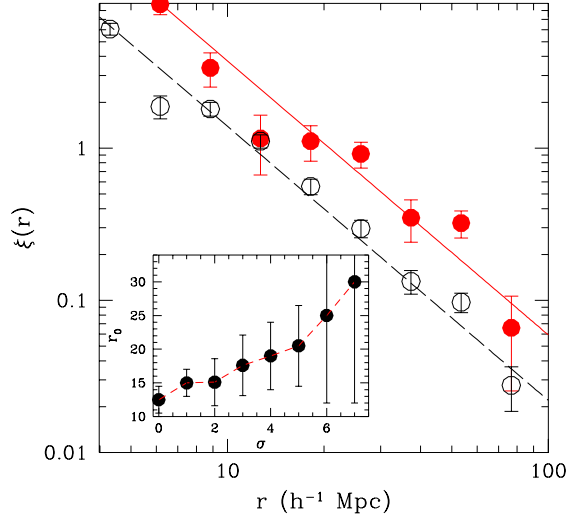


Figure 5. Two-point correlation function of all APM clusters (open symbols) and of $\sigma > 4$ clusters (filled symbols). The lines represent the best $(r/r_0)^{-1.8}$ fit with $r_0 \simeq 12$ and $\simeq 20 \ h^{-1}$ Mpc respectively. Inset: The cluster correlation length as a function of substructure significance.

the cooling flow clusters with high mass accretion rates (Loken, Melott & Miller [17]).

5. Supercluster - Cluster Alignments

We have applied a friends of friends algorithm to identify superclusters in the 3D distribution of APM clusters. We used various percolation radii and estimated for each supercluster the alignment signal, δ , estimated between the orientations of all member clusters. Furthermore we estimated the mean signal for superclusters of which all member clusters have substructure significance σ above a chosen threshold. In figure 6 (left panel) we see that there is a strong correlation between $\langle \delta \rangle$ and σ , corroborating the results of the previous section. In the right panel of figure 6 we present the frequency distribution of the misalignment angle, $\delta\phi$ for all superclusters with more than one member and the expected Gaussian for a uniform distribution. We see that indeed there is an excess at small $\delta\phi$'s. The hatched region shows the corresponding distribution for those superclusters having all their cluster members with substructure index $\sigma > 2$. It is evident that the distribution is even more skewed towards small $\delta\phi$'s.

We have already established, in section 3, that there is an alignment signal between nearby clusters (which is also an increasing function of cluster substructure significance). A further interesting question regarding large-scale alignment effects is whether clusters are also aligned with the orientation of their parent supercluster. To this end we have esti-

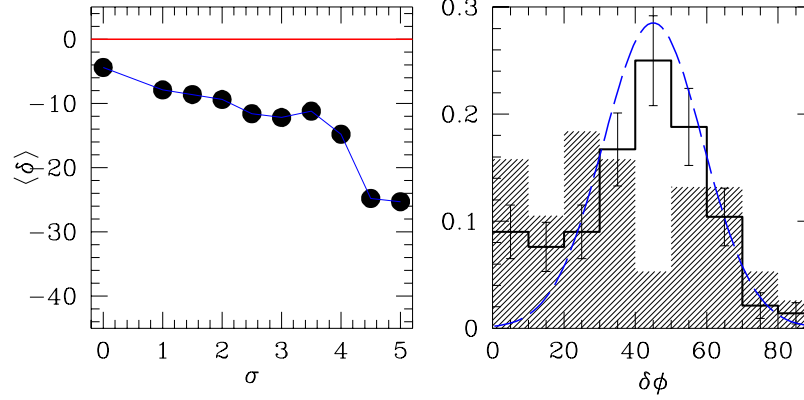


Figure 6. Left panel: Mean alignment signal between supercluster members versus substructure significance (note that here all members should have σ larger than the indicated limit). Right panel: Frequency distribution of all supercluster $\delta\phi$ values (histogram), of those that all member cluster have $\sigma > 2$ (hatched region) and the expected from a uniform distribution (continuous line).

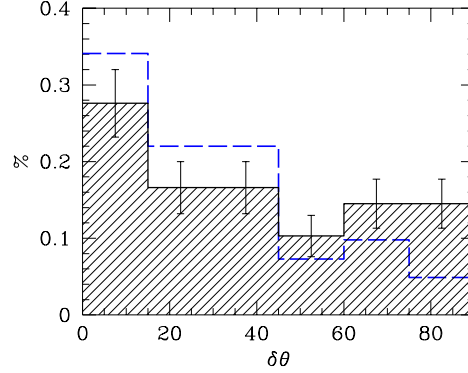


Figure 7. Frequency distribution of the misalignment angle between cluster members and their parent supercluster orientations. Broken line corresponds to superclusters with percolation radius of $30 h^{-1}$ Mpc while the hatched distribution to that with percolation radius of $20 h^{-1}$ Mpc.

imated the misalignment angle, $\delta\theta$ between the orientation of each supercluster, θ_s , with the mean position angle, $\langle\theta\rangle$, of its member clusters, i.e.; $\delta\theta = |\theta_s - \langle\theta\rangle|$. In figure 7 we present the frequency distribution of $\delta\theta$ for two different supercluster catalogues (based on percolation radii of 20 and $30 h^{-1}$ Mpc, respectively). The significant excess of small $\delta\theta$'s is evidence that indeed clusters do show significant alignments with the orientation of their parent superclusters.

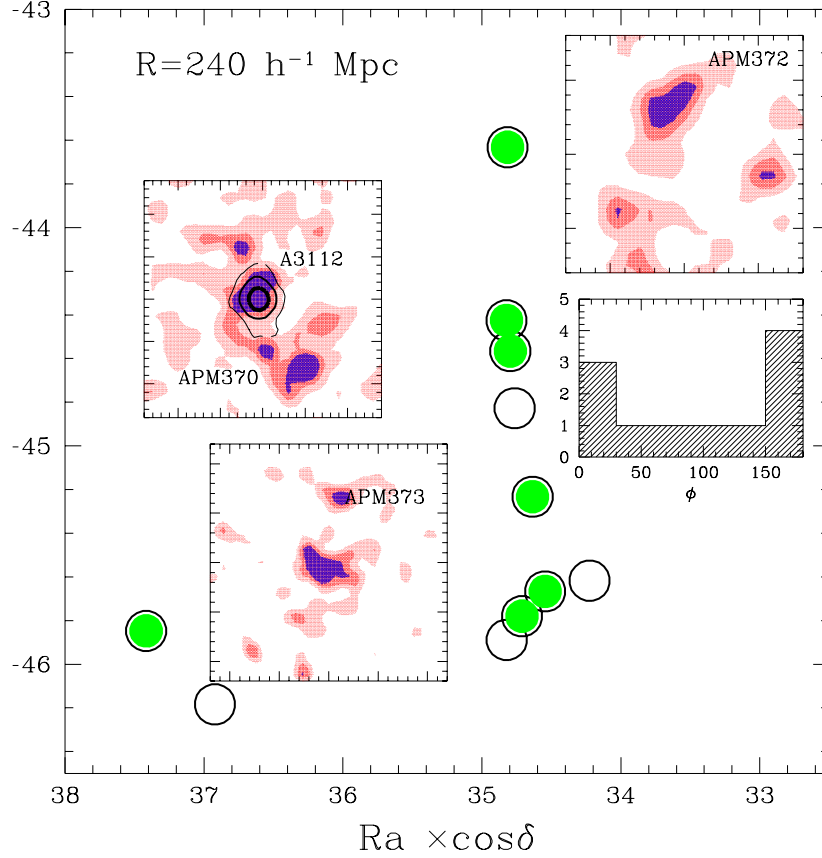


Figure 8. A filamentary APM supercluster containing A3112, A3104, A3111 as well as 9 poorer APM clusters. The percolation (linking) parameter is $12 h^{-1}$ Mpc. Filled dots represent clusters with substructure index $\sigma > 2.5$. There is a clear tendency of the cluster position angles to be preferentially aligned with the projected orientation of the supercluster.

As an individual illustration we present, in figure 8, a filamentary APM supercluster together with the smooth galaxy density distribution of some member clusters and the frequency distribution of all the member cluster position angles. It is evident that there is an excess of clusters with position angle orientation similar to that of the supercluster itself (note that filled dots represent clusters with significant substructure). For the A3112 cluster we overlay also the smooth ROSAT X-ray contours.

6. Conclusions

We have presented evidence, based on the large APM cluster sample, that there is a strong link between the dynamical state of clusters and their large-scale environment. Cluster near-neighbours are statistically aligned with each other and with the orientation of their parent supercluster. Furthermore, dynamically young clusters are significantly more aligned with their nearest neighbours and they are also much more spatially clustered. This supports the hierarchical clustering models in which clusters form by merging along the large-scale filamentary structures within which they are embedded.

Acknowledgments

I thank all my collaborators S.Basilakos, S.Maurogordato and C.Benoist for allowing me to present our results prior to publication.

References

- [1] Arnaud, M., Maurogordato, S., Slezak, E., Rho, J., 2000, A&A, 355, 848
- [2] Basilakos S., Plionis M., Maddox S. J., 2000, MNRAS, 315, 779
- [3] Bingelli B., 1982, AA, 250, 432
- [4] Bond, J.R., 1986, in *Galaxy Distances and Deviations from the Hubble Flow*, eds. Madore, B.F., Tully, R.B., (Dordrecht: Reidel), p.255
- [5] Bond, J.R., 1987, in *Nearly Normal Galaxies*, ed. Faber, S., (New York: Springer-Verlag), p.388 (Dordrecht: Reidel), p.255
- [6] Borgani, S. & Guzzo, L., 2001, Nature, 409, 39
- [7] Böhringer H., 1995, in Proceedings of the 17th Texas Symposium on Relativistic Astrophysics and Cosmology, eds. Böhringer H., Trümper J., Morfill G. E., The New York Academy of Sciences
- [8] Djorgovski, S., 1983, ApJ, 274, L7
- [9] Dalton G. B., Maddox S. J., Sutherland W. J., Efstathiou G., 1997, MNRAS, 289, 263
- [10] Durret, F., Forman, W., Gerbal, D., Jones, C., Vikhlinin, A., 1998, A&A, 335, 41
- [11] Evrard A.E., Mohr J.J., Fabricant D.G., Geller M.J., 1993, ApJ, 419, L9
- [12] Fuller, T.M., West, M.J. & Bridges, T.J., 1999, ApJ, 519, 22
- [13] van Haarlem, M., van de Weygaert, R., 1993, ApJ, 418, 544
- [14] Kampen van E., Rhee, G.F.R.N., 1990, A&A, 237, 283
- [15] Kolokotronis, V., Basilakos, S., Plionis, M., Georgantopoulos, I., 2001, MNRAS, 320, 49
- [16] Lacey, C., Cole, S., 1996, MNRAS, 262, 627
- [17] Loken, C., Melott, A.L., Miller, C.J., 1999, ApJ, 520, L5

- [18] Maddox S.J. , Sutherland W.J., Efstathiou G., Loveday, J. 1990, MNRAS, 243, 692
- [19] Mohr, J.J., Evrard, A.E., Fabricant, D.G., Geller, M.J., 1995, ApJ, 447, 8
- [20] Novikov, D. *et al.*, 1999, MNRAS, 304, L5
- [21] Onuora, L.I., Thomas, P.A, 2000, MNRAS, 319, 614
- [22] Plionis M., 1994, ApJS., 95, 401
- [23] Plionis M., 2001, in the proceedings of the *Clusters and the High-Redshift Universe observed in X-rays*, XXIth Moriond Astrophysics Meeting, eds. Neumann et al., *in press*
- [24] Plionis M., Basilakos, S., 2001, MNRAS, *submitted*
- [25] Richstone, D., Loeb, A., Turner, E.L., 1992, ApJ, 393, 477
- [26] Roettiger, K., Burns, J. & Loken, C., 1993, ApJ, 407, L53
- [27] Roettiger, K., Stone, J.M., Burns, J., 1999, ApJ, 518, 594
- [28] Sarazin, C.L., 1988, in *X-ray Emission from Clusters of Galaxies*, Cambridge Astrophysics Series, Cambridge Univ. Press.
- [29] Sarazin, C.L., 2001, in *Merging Processes in clusters of Galaxies*, eds. Feretti, L., Gioia, M., Giovannini, G., (Dordrecht: Kluwer).
- [30] Schindler S., 1999, in Giovanelli F., Sabau-Graziati L. (eds.), proceedings of the Vulcano Workshop 1999, *Multifrequency Behaviour of High Energy Cosmic Sources*, astro-ph/9909042.
- [31] Schindler S., 2000, in Giovanelli F., G. Mannocchi (eds.), proceedings of the Vulcano Workshop 2000, *Frontier Objects in Astrophysics and Particle Physics*, astro-ph/0010319.
- [32] (Schüecker, P., Boehringer, H., Reiprich, T.H., Feretti, L., A&A, *in press*, (astro-ph/0109030)
- [33] Splinter, R.J., Melott, A.L., Linn, A.M., Buck, C., Tinker, J., 1997, ApJ, 479, 632
- [34] Struble, M.F., 1990, AJ, 99, 743
- [35] Struble, M.F., Peebles, P.J.E., 1985, AJ, 90, 582
- [36] Trevese, D., Cirimele, G., Flin, P., 1992, AJ, 104, 935
- [37] West, M. J., 1989, ApJ, 347, 610
- [38] West, M. J., Villumsen, J.V., Dekel, A., 1991, ApJ, 369, 287
- [39] West, M. J., 1994, MNRAS, 268, 79
- [40] West, M. J., Jones C., Forman W., 1995, ApJ, 451, L5
- [41] Zabludoff, A.I. & Zaritsky, D., 1995, ApJ, 447, L21